NTHAS8: The Eighth Japan-Korea Symposium on Nuclear Thermal Hydraulics and Safety
Beppu, Japan, December 9-12, 2012

Paper Number N8P1113

NUMERICAL QUANTIFICATION OF DISSOLVED GAS BEHAVIOR IN PRIMARY COOLANT SYATEM OF FAST REACTOR - SUPPRESSION OF GAS ENTRAINMENT USING DIPPED PLATE -

Kenichiro ETO[1*], Akira YAMAGUCHI[1] and Takashi TAKATA[1], Hiroyuki OHSHIMA[2], Kei ITO[2]

[1]Graduate School of Engineering, Osaka University
2-1 Yamadaoka, Suita, Osaka, 565-0871 Japan
+81-6-6879-7895 eto_k@qe.see.eng.osaka-u.ac.jp

[2]Oarai Research and Development Center, Japan Atomic Energy Agency
4002 Narita, Oarai, Ibaraki, 311-1393, Japan
+81-29-267-4141 ito.kei@jaea.go.jp

ABSTRACT

When inert gas is present in the primary coolant of a sodium cooled fast reactor (SFR), it may cause a core power fluctuation or a reduction of heat transfer at an intermediate heat exchanger (IHX). Therefore, it is necessary to clarify an allowance level of the gas in the system design of SFR. In Japanese Sodium Fast Reactor (JSFR), a dipped plate (D/P) will be installed at the upper plenum so as to suppress a fluid fluctuation at the free surface and entrainment of argon (Ar) gas bubbles into the piping system. In the present study, an influence of the D/P on the gas behavior has been investigated using the VIBUL code. In the analysis, the upper plenum region is segmented into two parts through the D/P. The flow exchange rate is extrapolated based on the one-tenth water experiment. As a result, it is demonstrated that the entrainment of Ar gas is suppressed considerably by the D/P although the background void fraction, in which no Ar entrainment from the free surface is taken into account, increases comparing with that without D/P. The quantification of the allowance level of Ar entrainment is also investigated based on the computation result.

1. INTRODUCTION

In a sodium-cooled fast reactor, inert gases will exist in a primary coolant system either in a state of dissolved gas or free gas bubbles. There are two sources of the inert gas in the system; one is argon (Ar) and the other is helium (He).

Ar gas, used as a reactor vessel cover gas, exists on a free surface of the coolant at an upper plenum of the reactor vessel. The usage of the free surface is unavoidable because reservoir function is needed to absorb a thermal expansion of liquid sodium. Since the Ar cover gas exists above the free surface, it would dissolve into the liquid sodium and is dispersed in the primary coolant system by diffusion and advection. At the same time, free gas bubbles of Ar will flow into the liquid sodium by an entrainment at the surface caused by, such as, a break up surface wave due to fluctuation and a surface vortex.

He gas is produced as a result of disintegration of B_4C control rod material and is emitted as small bubbles to the reactor core. Even if these gases are dissolved in coolant at high temperatures, these are come out as bubbles in cooler part in the intermediate heat exchanger (IHX) (Winterton, 1972).

In Japanese Sodium-Cooled Fast Reactor (JSFR), studied by Japan Atomic Energy Agency (JAEA), an installation of a dipped-plate (D/P) is being planned at the upper plenum of the reactor vessel so as to suppress the fluid fluctuation and the surface vortex at the liquid sodium surface (Kimura, et al., 2006). The D/P will be installed at the upper plenum as shown in Fig.1. When the D/P is installed, the upper plenum is divided roughly into two volumes and exchange flow between the volumes also be suppressed. Consequently, the D/P will affect the inert gas behavior in terms of not only the suppression of the entrainment but also the diffusion and the advection of gas.

When gas bubbles are transported to the primary coolant system, they may cause a disturbance in reactivity, a nucleation site for boiling and cavitation, flow instability and so on. Therefore, the investigations

of inert gas behavior and its acceptance level are very important from the viewpoint of design and safety of the SFR. In order to evaluate the inert gas behavior numerically in the primary coolant piping system, a computational code VIBUL was developed (Berton, 1991). The numerical models of the bubble behavior at the upper plenum and the nucleation in the IHX have been modified to improve the prediction accuracy (Tatsumi, et al., 2008). In the present paper, an influence of the D/P on the inert gas behavior has been investigated numerically using the VIBUL code. An acceptance level of the gas entrainment has also been discussed based on a background concentration of gas caused by the He emission from the control rods and the resolution of Ar gas at the free surface.

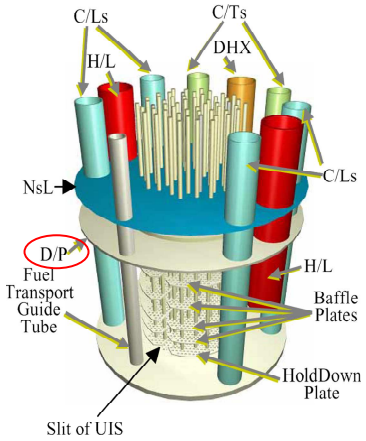

Fig. 1 D/P at upper plenum

2. NUMERICAL METHOD

2.1 Numerical Method in VIBUL Code

The VIBUL code was originally developed for dynamics of gas behavior in primary coolant system of a pool-type SFR (Berton, 1991) and modified by the authors for the loop-type JSFR design (Yamaguchi, et al., 2005). Important and key issues for predicting the gas bubble concentration in the SFR system are the models of the bubble source and sink terms. In the VIBUL code, the following models are implemented; a diffusion from bubble surface and free surface at the upper plenum, an entrainment and emission of gas bubble at the free surface, a generation at the control rod and a nucleation at the IHX.

The plant system is represented as a network of volumes and paths. The bubble number density as a function of the bubble size and the total amount of the gas are evaluated in each volume. The bubble radius range is divided into K groups according to a logarithmic scale as:

$$r_i = r_{\min} \times 10^{k(i-1)}, k = \frac{1}{K-1}\log_{10}\frac{r_{\max}}{r_{\min}} \quad (1)$$

Where r_i is the median radius of a bubble in group i, and r_{min} and r_{max} are minimum and maximum radii of the bubble size, respectively.

The total mass conservation of the gas bubble and dissolved state in a component of the system is expressed as:

$$V_{Na}\sum_{i=1}^{K} N_{bi}\frac{d}{dt}N_{mi} + V_{Na}\frac{d}{dt}N_d = -2\sqrt{\frac{Dv_h L}{\pi}}\left(N_d - H\ P_{FS}\right) - QN_d + Q\tilde{N}_d \quad (2)$$

where, $$H = \frac{S\times 10^{-5}\times \rho_{Na}}{M_{Na}} \quad (3)$$

Where N_b is the number density of bubbles, N_m is the molar mass of the gas in one bubble, and N_d is the mol concentration of the dissolved gas, V_{Na} is the coolant volume in the volume and Q is the volumetric flow rate of the coolant. The tilde (~) means the upstream value. D, v_h, L, H and ρ_{FS} are the diffusion coefficient of the gas in the sodium, the horizontal velocity at the free surface, the length of free surface, Henry's constant and the pressure of the cover gas should be P_{FS}, respectively. The diffusion coefficient D is given in (Reed, et al., 1970). S is the solubility, ρ_{Na} is the coolant density, M_{Na} is the mol concentration of coolant. The first term of the right side in Eq(2) reveals the diffusion of dissolved gas from the free surface.

The conservation of the number of density of ith group gas bubbles is shown in the following:

$$V_{Na}\frac{d}{dt}N_{b,i} = -\alpha_i V_{Na} N_{b,i} - QN_{b,i} + Q\tilde{N}_{b,i} + S_i \quad (4)$$

The first term of the right side means the emission from the free surface. α_i is the degassing constant and is calculated as:

$$\alpha_i = \frac{A_{Na} v_{t,i}}{V_{Na}} \quad (5)$$

Here, A_{Na} is an area of the free surface, and v_t is the terminal rising velocity of the bubble.

As concerns the source term S_i in Eq.(4), the entrainment from the free surface, the generation at the control rods, and the nucleation at the IHX. The first two sources are considered as input parameters.

Let us describe the nucleation model briefly. Since the primary coolant temperature decreases at the IHX due to a heat exchange towards the secondary coolant, a nucleation of gas appears on the heat transfer tube surface. The initial bubble radius R is described in the following equation:

$$P_G - P_L = \frac{2\sigma}{R} \quad \text{where} \quad p_G = \frac{N_d}{H} \quad (6)$$

P_G, P_L, and σ are the intrinsic bubble pressure, the flow pressure around the bubble, and surface tension.

When the initial gas bubble grows larger, the flow resistance increases. After that, when the gas bubble become certain size, the force balance, surface tension and lift force acting on bubble, is lost and the bubble is detached from tube surface (Hibiki, et al., 2005). In the VIBUL code, the radius of nucleation bubble is approximately 80μm with for Ar gas, 100μm for He gas. As the reason, He gas have more intrinsic pressure.

Then the mass conservation equation for a single bubble is given as:

$$\frac{dN_m}{dt} = -4k\pi r^2 \left[N'_d - N_d\right] \quad (7)$$

where, $$k = \frac{ShD}{r} \quad (8)$$

k is the coefficient of transporting gas between gas and sodium and Sh is Strouhal number (Crift, et al., 1978). N'_d is the molar gas of saturation solubility per unit time. Since saturation N'_d depends on the temperature and the pressure, these are to be parameters in Eq.(6).

2.2 Numerical Condition

Fig. 2 shows the node configuration of the JSFR primary piping system without the D/P. Each component, such as the upper plenum, the hot leg piping and so on, is modeled as a volume and is connected with paths. Since the He emission from the control rods appears at the inner core region, the core region is divided into two volumes.

With regard to the free surface, it exists in the upper plenum and the pump. It is noted that the dissolution of He at the free surface is ignored in the present analysis because the concentration of He in the cover gas would be negligibly-small.

In the D/P installation case, the upper plenum is segmented into two values as shown in Fig.3. The reason why "Upper plenum1" and "Upper plenum2" aren't connected paths, only two paths can be connected for one volume in VIBUL code. So, Numerical condition is necessary to set up as Fig.3. In the analysis, the influence of the D/P is considered by a flow exchange rate between the upper plenum volumes. The flow rate exchange is set to approximately 0.7% of the total flow rate based on one-tenth water experiment carried out by JAEA. (Kimura, et al., 2003) In the VIBUL code, the temperature and the pressure distributions in the piping system are treated as an input parameter as well as the flow rate. The rated operating condition is applied in the present analysis. The Ar and He sources are also input variables. The He emission rate from the control rods is set to be constant (0.4cc/sec with 50μm in radii, Yamaguchi et al., 2005). As concerns the Ar as bubble entrainment, the entrainment rate and its radii are treated as a sensitivity parameter in the present study.

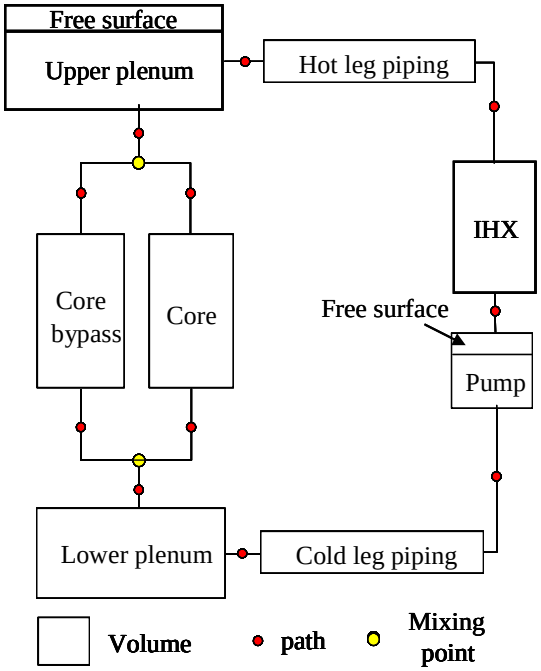

Fig. 2 Analytical nodes without D/P

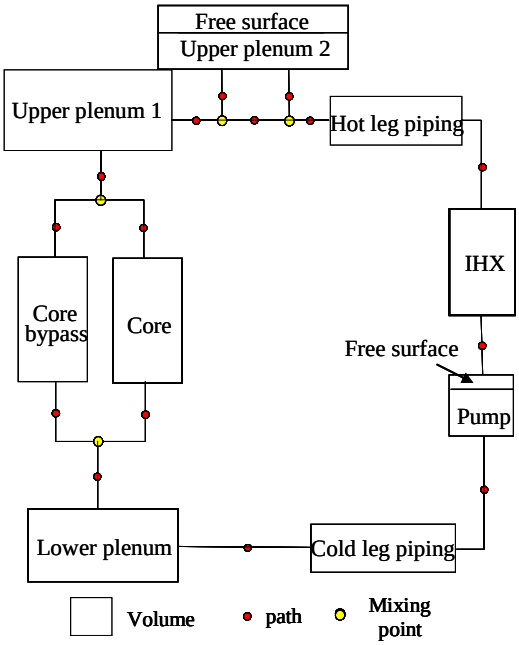

Fig. 3 Analytical nodes with D/P

3. RESULT AND DISCUSSION

3.1 Background Level of Gas Concentration

When the D/P is installed, a fluctuation of free surface at the upper plenum is suppressed. Thus the entrainment of gas bubbles will be reduced. Furthermore, the D/P will protect an inflow of gas bubbles inside the piping system because of its small flow exchange rate. At the same time, it also protects a release of gas generated inside the piping system (He at the control rod). Therefore, a background level of the gas concentration is investigated firstly. In the background level analyses, no Ar entrainment in a bubble form at the free surface of the upper plenum is assumed.

Fig. 4 shows the bubble number density of (a) Ar and (b) He at the core inlet, respectively. Figs. 5 and 6 also show the bubble concentration at the upper plenum inlet and the hot leg piping inlet, respectively.

As shown in Fig.4, the bubble number density increases when the D/P is installed. This is attributed to the fact that the bubble emission from the upper plenum free surface is suppressed by the D/P. The peak radius of the bubble is approximately 50μm in Ar and 70μm in He that comes from the nucleation at the IHX. On the other hand, it is described these bubble radii are 80μm and 100μm, respectively, in chapter 2. For the reason, gas bubbles are shrinked around sodium pressure at low place.

In the background condition, the void fraction at the core inlet is evaluated to 2.91×10^{-7} (Ar: 3.58×10^{-8} , He: 2.56×10^{-7}) without the D/P and 6.64×10^{-6} (Ar: 1.68×10^{-7}, He: 6.47×10^{-6})with D/P. It can be concluded that the He gas is dominant in case of the background condition.

In the plenum inlet, the distribution of the number density spreads widely comparing with that at the core inlet as seen in Fig. 5 because of the total pressure decrease. When the coolant flows into the upper plenum with the free surface (Upper plenum without the D/P and Upper plenum2 with the D/P, see Figs. 2 and 3), the number density in case of the D/P is smaller than that without the D/P as shown in Fig. 6. This is attributed to the fact that the characteristic height (Z_{Na}) becomes low of the volume segmentation. Thus more bubbles are released from the free surface in case of the D/P installation.

Since the He bubble is emitted at the core (0.4cc/s with 50μm in radius), the He bubble number density has two local peaks as shown in Fig. 6 (b).

Table 1 shows the proportion of the bubble release rate from the free surfaces at the upper plenum and the pump. As summarized in Table 1, the most of the bubbles are emitted from the upper plenum free surface when the D/P is not implemented.

Table.1 Release bubble proportion from free surfaces in background condition

	Argon gas		Helium gas	
	upper plenum	pump	upper plenum	pump
with D/P	84%	16%	31%	69%
without D/P	99%	1%	97%	3%

When the D/P is installed, the Ar bubble is emitted dominantly from the upper plenum free surface same as that without the D/P case. On the contrary, the He bubbles are emitted mainly from the pump free surface because the He is emitted to the core and it hardly flows to the free surface region of the upper plenum through the D/P. As mentioned above, the void fraction consists of the He bubble mostly (97% of the void fraction). Consequently, it is concluded that the bubble release from the pump will affect the background void fraction strongly.

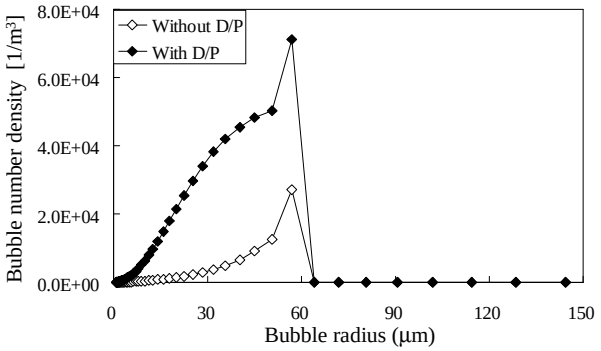

(a) Ar

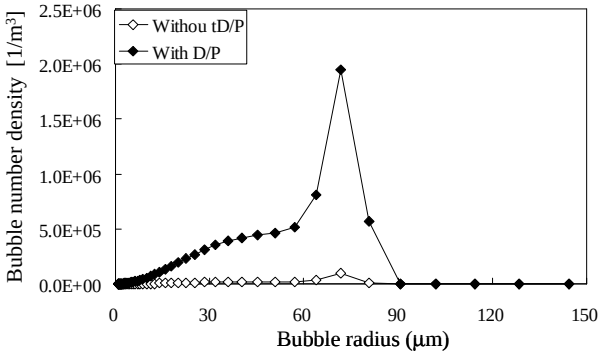

(b) He

Fig. 4 Bubble number density at core inlet in backgr ound condition

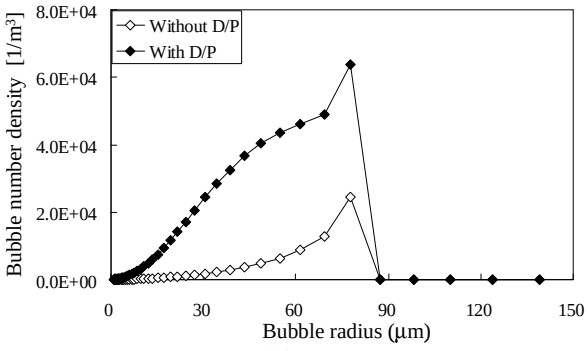

(a) Ar

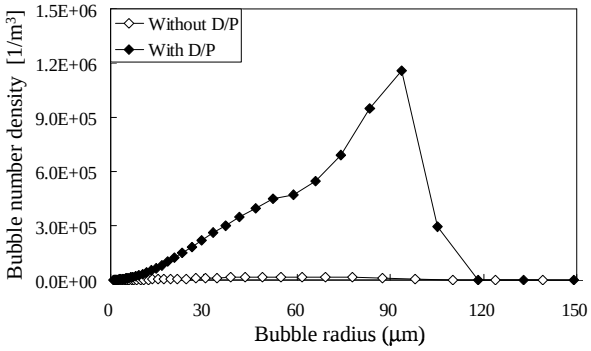

(b) He

Fig. 5 Bubble number density at upper plenum inlet background condition

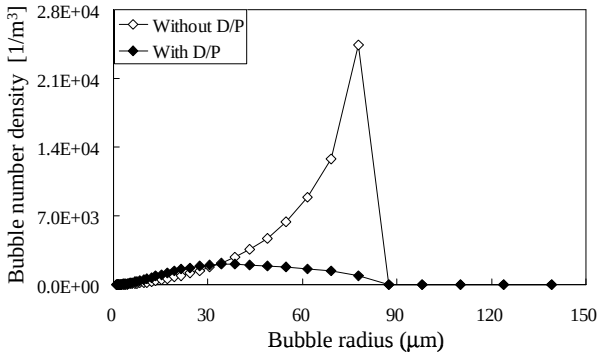

(a) Ar

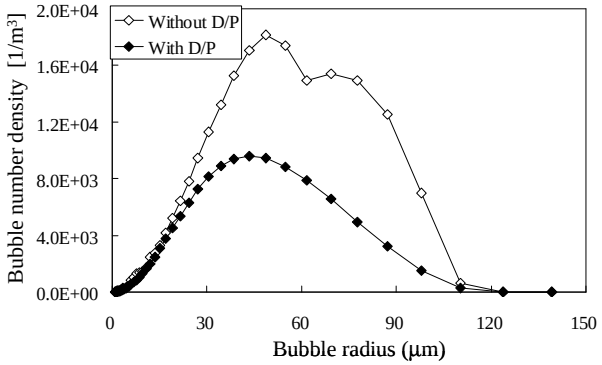

(b) He

Fig. 6 Bubble number density at upper plenum in background condition

3.2 Influence of Argon Bubble Entrainment

In order to investigate an influence of Ar bubble entrainment at the upper plenum free surface on the bubble concentration behavior in the piping system, sensitivity analyses are carried out. In the analyses, a constant entrainment rate of Ar (4cc/s), which is reasonably conservative in case of no D/P (Yamaguchi, et al., 2005) is assumed 4cc/s and the radius of the bubble is chosen as a parameter (50 and 100μm).

Fig. 7 shows the Ar bubble number density at the core inlet when the Ar bubble radius is set to 50μm.

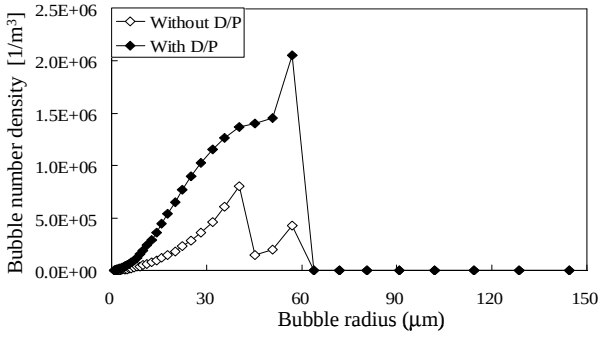

Fig. 7 Ar bubble number density at the core inlet (Ar: 4.0cc/s, 50μm in radius)

In the case of no D/P installation (Without D/P), the bubble number density has two local peaks as in Fig. 7. Comparing with that in the background condition (Fig. 4(a)), it is apparent that the first peak (approximately 40μm) comes from the entrainment at the upper plenum. On the other hand, the number density increases overall and an obvious density peak due to the entrainment does not appear when the D/P is installed. As a result, the increase of the void fraction caused by Ar gas is evaluated to 9.77×10^{-7} in case of no D/P and 4.03×10^{-6} in case of the D/P installation.

Fig. 8 shows the Ar bubble number density at the upper plenum. Since the flow exchange rate is too small in case of the D/P installation, the number density distribution changes quite a bit. As seen in Fig. 8, the number density of large radius (>60μm) decreases dramatically caused by the emitting from the free surface.

When the D/P is installed, the entrained Ar gas flows hardly into the hot leg piping system in a bubble form because of the small flow exchange rate via the D/P. At the same time, the more dissolution of Ar gas will take place at the upper plenum between the D/P and the free surface. The dissolved gas can flow into the piping system. Once it flows inside the D/P, it is not easy to release to the cover gas of the upper plenum. Consequently, the void fraction becomes higher in case of the D/P installation than that without the D/P as shown in Figs. 7 and 8.

It is concluded that the D/P installation increases the void fraction in the primary coolant piping system when the same amount of the gas entrainment is assumed. That is why the emission of gas bubbles from the free surface decrease. However, it is also carefully mentioned that the D/P plays an important role for suppressing the amount of the entrainment.

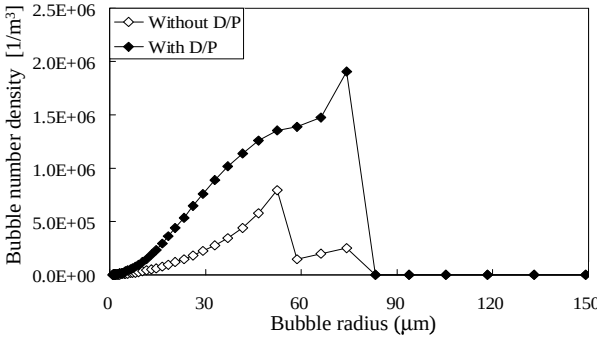

(a) Upper plenum inlet

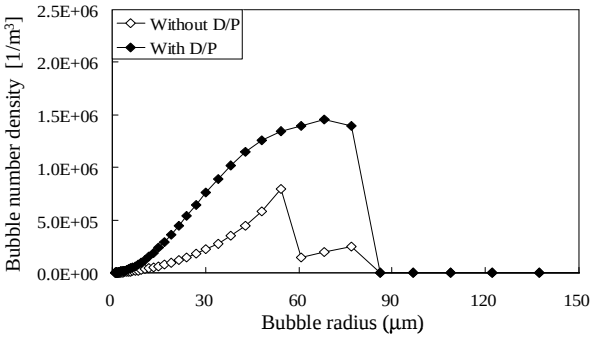

(b) Hot leg piping inlet

Fig. 8 Ar bubble number density at upper plenum (Ar: 4.0cc/s, 50μm in radius)

Fig. 9 shows the Ar number density at the core inlet when the entrained bubble size becomes large (100μm).

Comparing with that in case of 50μm (Fig. 7), the number density decreases as in Fig. 9. The increase of the Ar gas void fraction is 1.61×10^{-6} and 7.51×10^{-6} from the background level in case of no D/P installation and D/P installation, respectively.

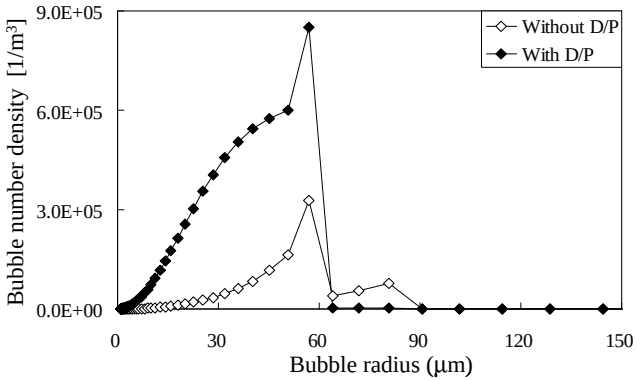

Fig. 9 Ar bubble number density at core inlet (Ar: 4.0cc/s, 100μm in radius)

As the entrained Ar gas is 100μm in radius, the local peak due to the entrainment shift from around 50μm to 80μm in case of no D/P installation. On the other hand, almost no number density is appeared at 80μm when the D/P is installed. This is attributed to the fact that the large bubble is emitted easily from the upper plenum surface as mentioned before.

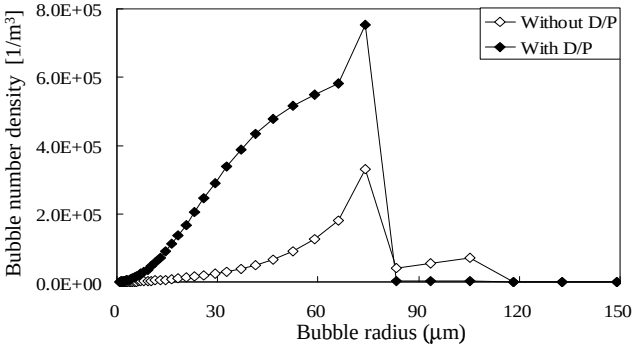

(a) Upper plenum inlet

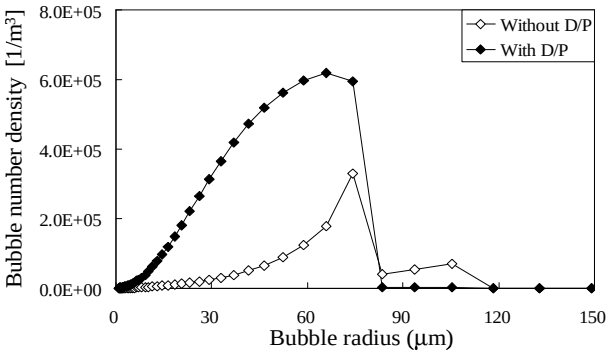

(b) Hot leg piping inlet

Fig. 10 Ar bubble number density at upper plenum (Ar: 4.0cc/s, 100μm in radius)

The number density of Ar bubble at the upper plenum is indicated in Fig. 10. The bubble behavior from the upper plenum inlet to the hot leg piping inlet is same with that in 50μm condition as seen in Fig. 8. When the entrained bubble size becomes large, the emitting rate from the free surface increases because of the rise of the terminal velocity. Furthermore, the amount of dissolution gas to the coolant is decreased because the bubble inner pressure decreases. Accordingly, the void fraction will decrease when the entrained bubble size enlarges. In other words, the void fraction will increase more as the entrained bubble size becomes smaller even when the total amount of the entrainment is same.

3.3 Consideration of Acceptable Bubble Entrainment

As mentioned in Sec. 3.2, the void fraction in the coolant will increase when the D/P is installed under the same amount of Ar bubble entrainment. At the same time, the D/P suppresses a coolant velocity and a fluctuation at the free surface resulting in a considerable decrease of the bubble entrainment (Ezure, et al., 2008). Consequently, an applicability of the D/P installation is investigated numerically by comparing the acceptable bubble entrainment rate. In the investigation, we assume 5% of the background condition with the D/P (3.3×10^{-7}) as an acceptance level tentatively. In the analysis, the entrainment rate is varied until the void fraction at the core inlet exceeds the acceptance level in each bubble size (30, 50 and 100μm). The acceptable entrainment rate is shown in Fig. 11.

As shown in Fig. 11, it is apparent that the acceptable entrainment rate in case of the D/P is smaller than that without the D/P. However, it is also concluded that remarkable reduction of the entrainment is not required in case of the D/P installation to achieve the same acceptance level as seen in Fig. 11. For instance, a smaller void fraction can be achieved when the entrainment rate reduces to lower than approximately one-fourth by the D/P in case of bubble with 50μm in radius. From the viewpoint of the control of bubble entrainment at the free surface of the upper plenum, it could be concluded that the D/P has the applicability to reduce the void fraction in the primary coolant system although the background void fraction will increase. It is again mentioned that an effective bubble emitting system at such as the IHX and the pump has a potential to reduce the background void fraction significantly.

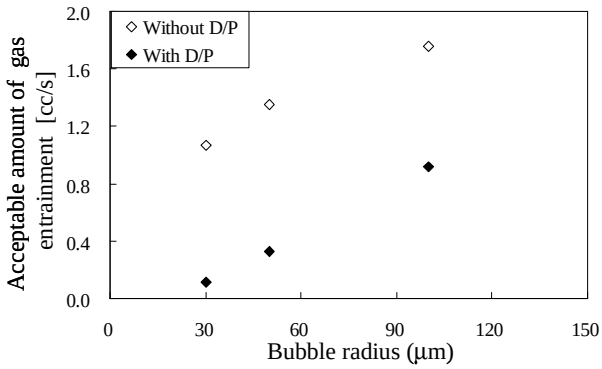

Fig. 11 Acceptable amount of Ar gas entrainment from upper plenum free surface

4. CONCLUSION

In the present study, we investigate the effect of the D/P on the bubble behavior using VIBUL code. As a result, it is demonstrated that the background void fraction rises in case of the D/P installation. Since the D/P suppresses the flow exchange, the bubble emission from the upper plenum free surface is also suppressed. At the same time, it is found that the bubble release from the pump free surface will affect the background void fraction strongly when the D/P is implemented.

When the same amount of the gas entrainment is assumed at the upper plenum, the D/P installation increases the void fraction in the primary coolant piping system comparing with that without the D/P. As the entrained bubble size becomes large, the emitting rate from the free surface increases due to the rise of the terminal velocity and the dissolution rate decreases because the bubble inner pressure is reduced. Consequently, the increase of the void fraction is suppressed when the bubble size becomes large. In this time, bubbles nucleated at IHX are majority and the amount of bubbles entrained from the free surface is negligibly small at the core inlet. Therefore, it is important to release the nucleation bubbles from the free surface of pump so that much bubble does not enter the core inlet in D/P installation case.

In the consideration of the acceptable bubble entrainment at the upper plenum where 5% of the background condition with the D/P is assumed, as the acceptable level, it is concluded that the acceptable entrainment rate decreases to approximately one-forth caused by the D/P installation. However, the entrainment rate can be reduced remarkably by the D/P. Consequently, it can be said that the D/P installation still has a potential to reduce the void fraction in the primary cooling system.

NOMENCLATURE

A_{Na}	area of free surface	[m^2]
D	diffusion coefficient of the gas	
H_d	Henry constant	[mol/s/Pa]
k	mas transfer coefficient	[m/s]
L	the length of free surface	[m]
M_{Na}	molar mass of sodium	[kg]
N_b	number density of bubbles	[$1/m^3$]
N_d	molar concentration of the dissolved gas	[mol/m^3]
N'_d	molar gas of saturation solubility per unit time	[mol]
N_m	molar mass of the gas in a bubble	[mol]
P_G	intrinsic bubble pressure	[Pas]
P_L	the flow pressure	[Pas]
P_{FS}	presser of cover gas	[Pas]
Q	volumetric flow rate of the coolant	[m^3/s]
r	median radius	[m]
S	solubility	[Pa^{-1}]
Sh	Strouhal number	[-]
S_i	volume of insert gases	[m^3]
v_h	horizontal velocity at the free surface	[m/s]
v_t	terminal velocity	[m/s]
V_{Na}	sodium volume in the plenum	[m^3]

Greek Letters

α_i	degassing constant	[m^2/s]
σ	surface tension	[kg/s^2]
ρ_{FS}	coolant density	[kg/m^3]

REFERENCES

Berton, J.L. ‘’Um modèle de calcul de la voe des bulles en réacteur,’’ NTCEA, SSAE, LSMI91, 023 in 1991, 1991.

Clift.R, et al., “Bubbles, drops, and particules” cademic Press 1978, 1978.

Ezure T., N. Kimura, et al., “Experimental Investigation on Gas Entrainment in Reactor Vessel Using 1/1.8th Scal Model – Evaluation of Onset Condition under Low Liquid Level Condition at Startup Operation -”, JAEA-Research 2009-021, 2009.

Hibiki T., et al., “Bubble Lift-off Size in Forced Convective Subcooled Boiling Flow” International Journal of Heat and Mass Transfer, 47, 3659-3667, 2004

Kimura N., et al., “Evaluation on Gas Entrainment in Reactor Vessel using 1/1.8th Scaled Model”, JAEA-Research 2006-067, 2006

Kimura N., et al., “Hydraulic Experiment for Compact Reactor Vessel - Measurement of Flow Field and Flow Optimization in Upper Plenum –“, JAEA-Research 2003-032, 2003

REED E.L., et al., “Solubility and diffusivity of Inert Gases in Liquid Sodium, Potassium and Na K” Liquid Metal Engineering Center. Report LMEC-69-36 Jan. 31, 1970, 1970.

Tatsumi E., et al., “Rationalization of Gas Entrainment Allowance Level at Free Surface of Sodium-Cooled Fast Reactor” NTHAS-5 in 2008, 2008.

Yamaguchi A., et al., “A Computational Model for Dissolved Gas and Bubble Behavior in the Primary Coolant System of Sodium-Cooled Fast Reactor,” 11th International Topical Meeting on Nuclear Reactor Thermal-Hydraulics, France, October, 2005, 477, 2005.

R.H.S. Winterton, Cover-gas bubbles in recirculating sodium primary coolant, Nuclear Engineering and Design, Volume 22, Issue 2, October 1972, Pages 262, 271, 1972.